Proceedings of the 1984
Winter Simulation Conference
S. Sheppard, U. Pooch, D. Pegden (eds.)

DIRECT ASCENT, DEEP SPACE INTERCEPT MODEL

Mark M. Mekaru
Air Force Institute of Technology
Wright-Patterson AFB, OH 45433

Richard C. Barclay
HQ Space Command
Colorado Springs, CO 30914

ABSTRACT

A stochastic computer model was developed to analyze a direct ascent, deep space intercept system. There are two error sources within the system: the deep space tracking system and the launch vehicle guidance system. The errors are modeled based on equipment performance data and analytical results. To compensate for the system errors, the requirements for a maneuverable intercept vehicle are developed. The requirements are described in terms of sensor acquisition distance and vehicle velocity change. Analyses of error sources and tradeoffs amongst maneuver factors are discussed.

INTRODUCTION

A stochastic computer model was developed to analyze a direct ascent, deep space intercept system. When launched, the direct ascent system goes through two phases of flight. The first phase involves boosting the intercept vehicle to a given altitude on board a launch vehicle. At burnout, the point when the launch vehicle propellant is depleted, the first phase ends, and the second phase begins with the intercept vehicle continuing in free flight. As the intercept vehicle approaches the deep space object, it detects the object with its sensor subsystem and maneuvers to intercept the object. The overall performance of the direct ascent, deep space intercept system is dependent upon how well the intercept vehicle can account for the errors in the overall system. There are two error sources in the system, and they both produce uncertainty in the intercept position.

The first error source is the deep space tracking system. One of the objectives of the tracking system is to locate objects and predict their future positions. For this paper, we consider only objects in deep space whose orbital period is greater than 225 minutes. At these distances, current deep space tracking systems can determine the position of these objects within 1-10 km on the average. However, the position uncertainty of the deep space object could be as large as 200 km.

The second error source in the system is the launch vehicle guidance subsystem. The launch vehicle boosts the intercept vehicle to a planned position. This serves as the initial position and velocity for the free flight of the intercept vehicle. Because of inaccuracies in the launch vehicle guidance subsystem, the actual position of the intercept vehicle at burnout will differ from the planned position. Additionally, the initial velocity of the intercept vehicle will likely differ from the planned velocity. These errors in initial conditions are propagated throughout the entire free flight of the intercept vehicle. The result is an error in the final position of the vehicle causing the vehicle to miss the intercept position.

For a successful intercept to occur, the tracking and guidance errors must be reduced. This can be achieved by improving tracking and guidance systems. However, another means to compensate for these errors is to allow the intercept vehicle to maneuver. The intercept vehicle would detect the deep space object as it approached it and would execute appropriate maneuvers to correct for position error. In this paper, a maneuvering intercept vehicle is considered.

The direct ascent, deep space intercept model incorporates the significant performance factors and simulates operational scenarios. The resulting data enables tradeoff analyses amongst improvements in tracking errors, guidance errors and intercept vehicle performance requirements.

ANALYTICAL MODEL

The astrodynamics applied in this model uses a two-body model. To determine the nominal trajectory for the intercept vehicle from the launch vehicle burnout to the intercept position, the "Gauss problem" algorithm is used. Given the initial and final position vectors, R1 and R2, the desired time of flight and the direction of flight, the Gauss algorithm computes the velocity vectors at R1 and R2. To obtain the velocity vectors, the eccentric anomaly is estimated and the time of flight is calculated. The computed time of flight is compared with the desired time of flight. If the difference is not within an acceptable tolerance, the eccentric anomaly value is modified until the flight time difference is acceptable. Based on the eccentric anomaly that yields an acceptable computed time of flight, the velocity vectors are computed. The velocity vectors are used to define a unique trajectory. Details of the algorithm are described in reference (1).

The first position vector, the point where the intercept vehicle begins free flight is in reality uncertain. This results in the intercept vehicle trajectory deviating from the planned or nominal trajectory. To determine the error in the final position and velocity vectors, a Kepler problem algorithm is used. Given the initial position and velocity vectors and time of flight, the Kepler algorithm predicts the final position and velocity vectors. The Kepler algorithm uses estimated values of universal variables to compute the time of flight. When the computed time of flight and desired time of flight difference is acceptable, the final position and velocity vectors are calculated. The details of the Kepler algorithm are described in reference (1). The error problem is compounded when the second position vector, the point where the space object was projected to be, is also uncertain.

The uncertainties are modeled as trivariate normal distributions based on performance data from launch vehicle guidance subsystem tests and on tracking data analysis. The actual development of these errors is accomplished by generating three random numbers from a standard normal distribution for the radial-tangential-normal components (6). The values are scaled by multiplying each by its respective input error characteristic. The space object errors are represented by the standard deviation predominantly "along the trajectory" (3). Finally the errors are transformed from the radial-tangential-normal coordinate system to the geocentric-equatorial coordinate system. The conceptual model is illustrated in Figure 1.

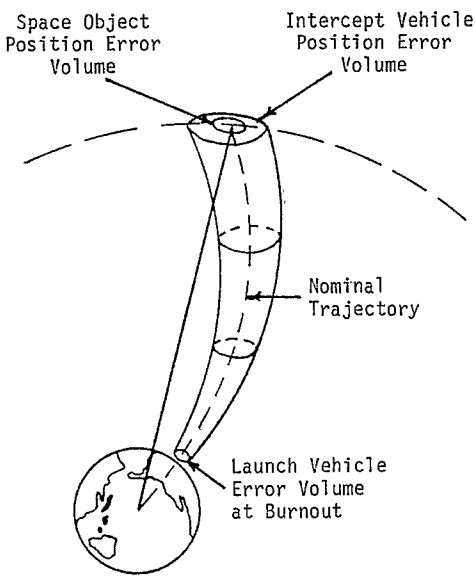

Figure 1. Conceptual Model

The difference between the planned or nominal trajectory and the error induced trajectory is called the missed distance. The magnitude of the missed distance which can be compensated by the intercept vehicle is dependant on the distance the vehicle sensor subsystem can acquire the space object and the maneuver capability of the vehicle. To determine the acquisition range, the space object is assumed to be a 300° K black body, Lambertian source, with a one square meter emitting area. Using a nominal infrared detector subsystem, acquisition distances as great as 2000 km are possible before the signal to noise ratio falls below a conservative value of 10 db. The flight path of the intercept vehicle is altered by changing the vehicle velocity ΔV. The amount of velocity change, ΔV, required is a function of the miss distance and the distance between the vehicle and the object. To determine the required ΔV, the vehicle trajectories are approximated as straight lines and similar triangle calculations are used. Figure 2 illustrates the similar triangle application. Based on the analytical models described in this section, the computer model is developed.

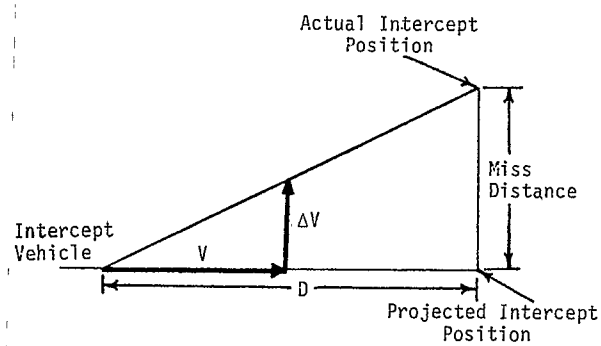

Figure 2. Similar Triangle Approximation for ΔV

COMPUTER MODEL

The direct ascent, deep space intercept computer model was written in FORTRAN 5 and was developed on a CDC Cyber. Figure 3 shows the structure of the program. The user inputs are: burnout position (R1), intercept position (R2), time of flight (TOF), error characteristics for the launch vehicle position (SCALR) and velocity (SCALV), and error characteristics for the space object position (SCALT) and velocity (V2T).

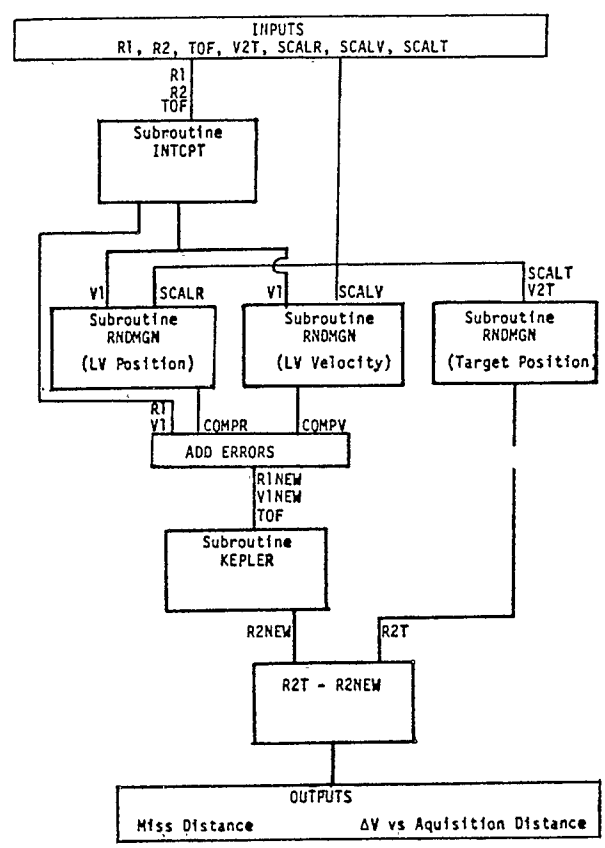

Figure 3. Computer Program Model

There are three major subroutines. INTCPT computes the nominal intercept trajectory. RNDMGN generates errors in the burnout position (R1), the burnout velocity (V1), and the space object position (R2) at the intercept point. KEPLER computes the interceptor position (R2) and velocity (V2). As part of the program, miss distance between the space object position and intercept vehicle position is calculated.

Subroutine INTCPT implements the Gauss problem algorithm. It uses R1, R2 and TOF to compute a nominal intercept trajectory and determines the velocity vectors, V1 and V2, associated with the two positions. Because of the transcendental nature of the equations in this algorithm, numerical iteration is required. Within, INTCPT, a disection technique is used to iterate to the proper universal variable, z. Bisection simply involves defining a specific interval for the variable value and checking the function value at the midpoint. The appropriate half is selected and a new midpoint value is used until a convergence interval is achieved (5:241).

The bisection method was selected because a well defined interval, 0 to $(2\pi)^2$, for the universal variable is known for the trajectory assumptions used in this paper. Additionally, convergence to within a specified interval is guaranteed when the initial interval is known and the number of iterations specified (4:95). INTCPT has thirty iterations and an initial interval of $39_8478418$ which assures convergence within 3.7×10^{-8}.

Following INTCPT, RNDMGN generates errors in R1, V1 and R2. Since the Cyber generates random numbers from a uniform distribution, RNDMGN applies the Central Limit Theorem to obtain a standard normal distribution. Three numbers are generated, one for each radial-tangential-normal component. Each number is scaled by the input error parameter, 1-σ. The resultant errors are converted to the geocentric-equatorial system and added to the appropriate vectors, R1, V1, and R2, to simulate errors.

KEPLER implements the Kepler problem algorithm. It uses the new R1, V1 and the original TOF to compute the error induced R2 and V2 for the interceptor. Numerical iteration is required in KEPLER to obtain the value of the universal variable, x. In this case, a Newton iteration scheme was chosen since there is not a well defined interval on the TOF vs. x curve. The Newton iteration scheme uses the slope of the curve at point x and the deviation from the desired TOF to determine the next x value (4:87, 1:198).

The miss distance is determined by the magnitude of the vector difference between the error induced space object position and the error induced interceptor position. Given the mean miss distance, the ΔV vs. acquisition distance is determined for distances of 250, 500, 1000, 1500 and 2000 km.

To assure that steady state conditions were achieved, 2500 iterations of the error generation segment of the model were executed. Steady state conditions were considered achieved when the miss distance changed less than five percent with additional iterations. It was determined that 500 iterations were sufficient to reach steady state. Therefore, the error generations are repeated 500 times to compute a mean miss distance. To determine the statistical consistency of the results, the variance for the mean miss distance was computed.

MODEL APPLICATIONS

Four hypothetical space objects were considered. Three of the objects were in equatorial geosynchronous orbits. Object A was stationed over 100 degrees West Longitude, Object B was stationed over 30 degrees East Longitude and Object C was stationed over 120 degrees East Longitude. The fourth object was in a semisynchronous orbit inclined 64 degrees with an eccentricity of 0.7 and perigee located in the Southern Hemisphere at 64 degrees. Burnout for launches for the geosynchronous objects occurred at 100 nmi. altitude and 34.5 degrees North Latitude, 120 degrees West Longitude, when the 120 degree meridian was aligned with the vernal equinox direction.

Error characteristics for the inertial guidance system (IGS) were derived from some of the most widely used systems. Table 1 depicts the error components in a radial-tangential-normal (R-T-N) coordinate system. Because of the apparent lack of correlation between the error terms, the guidance errors were modeled as spherically symmetric and represent a generic IGS. Figure 4 compares the performance of the generic TGS with actual IGS's for a four hour time of flight for Object A.

Table 1.
Injection Errors (1 sigma)
with Burnout Velocity 35,000 fps.

Radial Tangential Normal	Carousel V	Centaur Platform	Agena AGS	Units
R	2664	4460	2493	ft
T	7206	5412	4430	ft
N	6841	6313	4426	ft
$\dot{R}$	8.024	4.960	9.49	fps
$\dot{T}$	4.270	5.204	3.31	fps
$\dot{N}$	3.117	8.130	7.21	fps

The space tracking errors were also modeled in the radial-tangential-normal coordinate system. While tracking accuracy estimates vary for different objects due to location and sensor coverage, most of the object position error is along the trajectory Based on space tracking experts the space object position errors are modeled as a normal distribution in the tangential component and an order of magnitude less in the normal and radial components. Finally, the space object's velocity vector was obtained from the target's orbital perameters.

ANALYSIS

A performance baseline was established by comparing the miss distance as a function of IGS accuracy for a four hour time of flight for Object A. Figure 5 illustrates the baseline performance. From this baseline, four generic classes of IGS errors were selected: IGS-1 (baseline of 2.4×10^{-4} for each of six components), IGS-2 (1.32×10^{-4}), IGS-3 (5×10^{-5}) and IGS-4 (2.4×10^{-5}). The space tracking error classes for the analyses are 1, 5, 10, 20, 50 and 100 km, 1-sigma tangential.

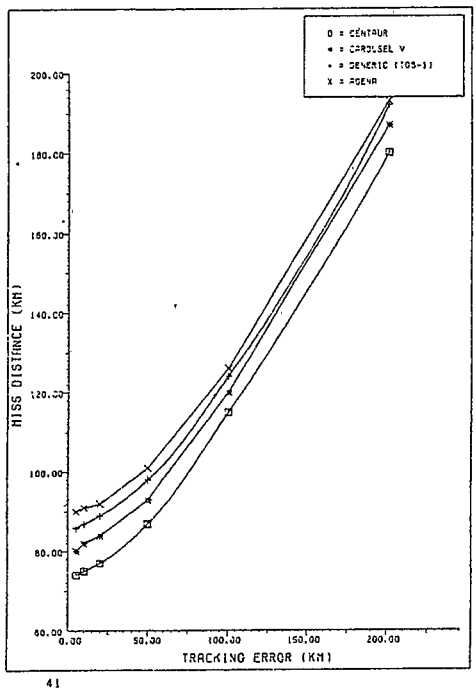

Figure 4. Comparison of Generic IGS with Actual Systems (Space Object A and 4 Hour TOF)

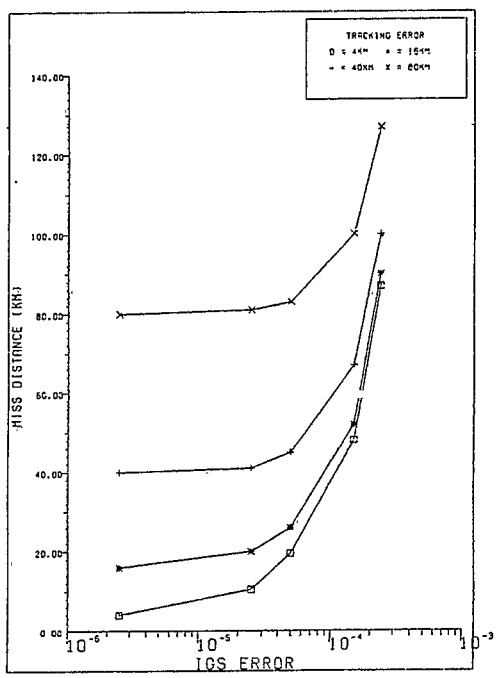

Figure 5. Generic Classes of IGS Performance (Space Object A and 4 Hour TOF)

Using these error classes, miss distance as a function of IGS accuracy and as a function of tracking accuracy were determined. Figure 6-9 graph the results for the four space objects and a three hour time of flight. The following inferences are made from these results:

1. If the IGS is limited by other factors to no better than 10^{-4} (1-σ across all components of position and velocity), there is no payoff for improving tracking from 10KM to 1KM, and very little payoff from 20KM to 1KM. That conclusion can be drawn due to the closeness of the 1, 5, 10, and 20KM lines in Figure 6a and the leveling off of the top two curves of Figure 6b.

2. If the space objects have tracking errors in excess of 50KM (1-σ tangential), relatively limited payoffs are possible with an improved IGS. This can be seen in the closeness of the IGS lines in Figure 6a and the leveling of the 50 and 100KM curves in Figure 6a.

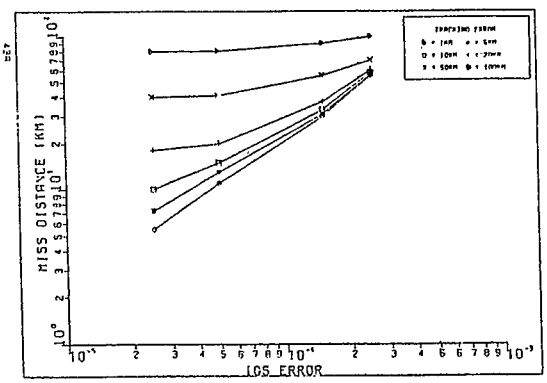

Figure 6a

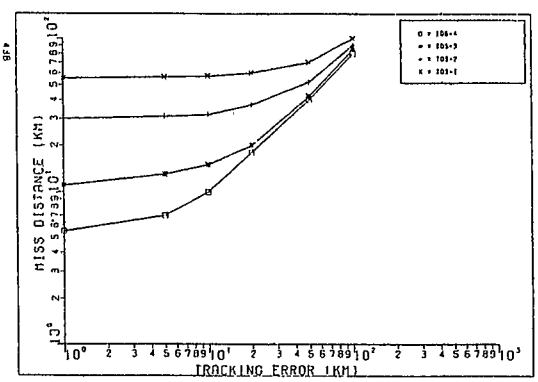

Figure 6b

Figure 6. System Performance for Space Object A and 3 Hour TOF

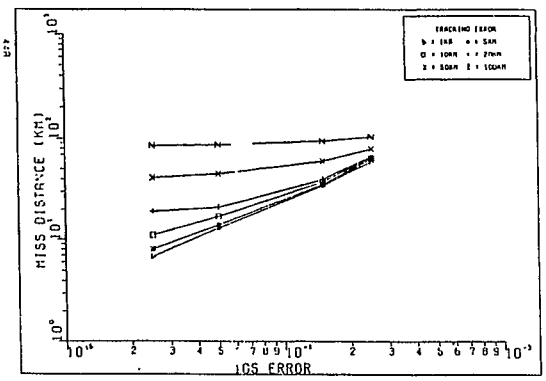

Figure 7a

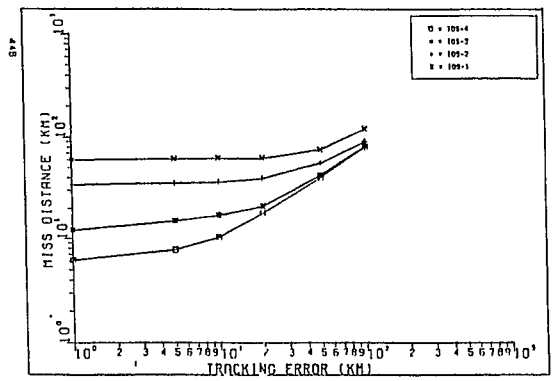

Figure 7b

Figure 7. System Performance for Space Object B and 3 Hour TOF

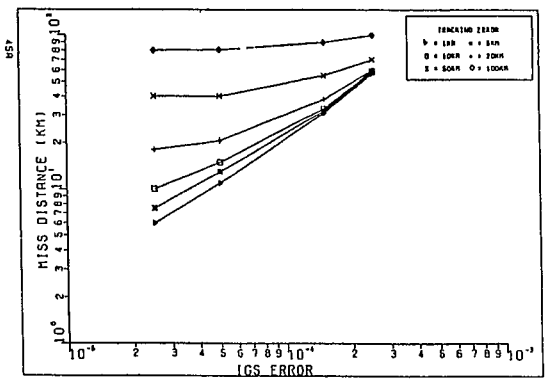

Figure 8a

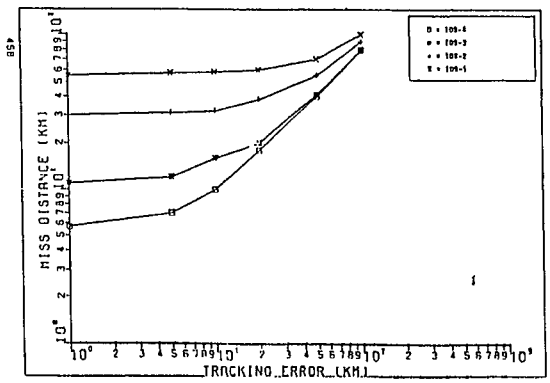

Figure 8b

Figure 8. System Performance for Space Object C and 3 Hour TOF

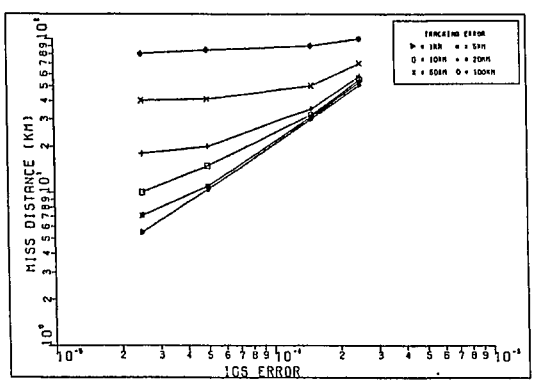

Figure 9a

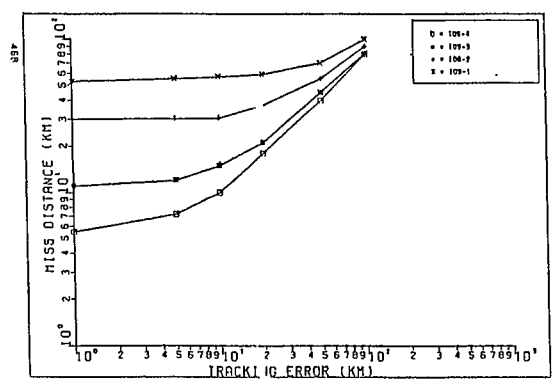

Figure 9b

Figure 9. System Performance for Space Object D and 3 Hour TOF

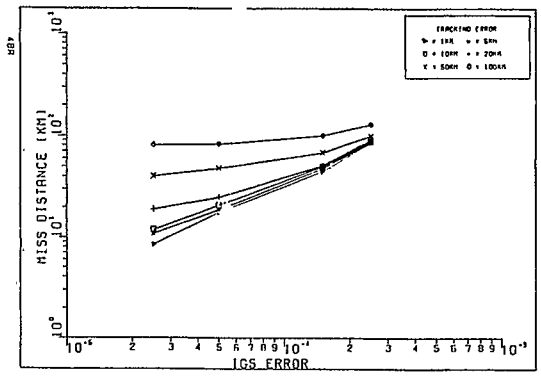

Figure 10a

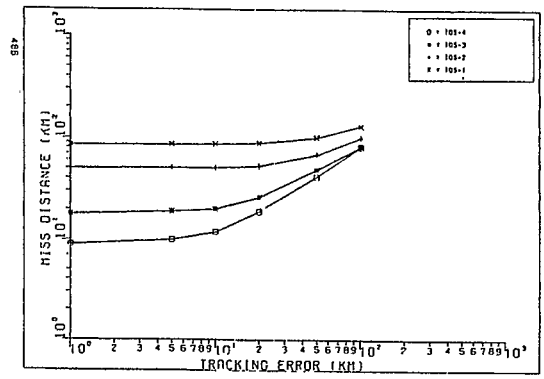

Figure 10b

Figure 10. System Performance for Space Object A and 4 Hour TOF

The time of flight to Object A was changed from three hours to four hours. Figure 10 is a graph of the results. This variation shows that miss distance has a greater sensitivity to a one hour time of flight change than to large differences in space object position errors.

Another insight into the system can be gained from analyzing the intercept vehicle velocity change, ΔV, as a function of sensor acquisition distance for different IGS accuracies. Figure 10 is a graph of these relationships. From the graph, one can conclude that limited payoffs are achieved with an improved IGS when the tracking errors are in excess of 50KM (1-σ, tangential).

TRADEOFF SCENARIOS

System tradeoff studies can be accomplished by using the intercept vehicle velocity change, ΔV, as a metric. The ΔV is used in the rocket equation to solve for the mass of the propellant needed to achieve the required velocity increment.

Scenario 1. IGS-1 and IGS-2 were considered with a 100 km sensor. Using an intercept vehicle with an initial mass of 500 kg and a nozzle exit velocity of 3km/sec, the required ΔV for the four space objects are shown in Table 2. The rocket equation was used to determine the propellant mass:

$$\frac{\Delta V}{V_e} = \ln \frac{M_i}{M_f}$$

where ΔV is the velocity increment change
V_e is the exit velocity of exhaust gases from the nozzle
M_i is the initial vehicle mass
M_f is the final vehicle mass

Considering the largest ΔV requirements, IGS-1 will require 30 kg of propellant and IGS-2 will require 19 kg. Since the difference is probably inconsequential, other factors such as reliability, cost and risk might be considered in the tradeoff between IGS-1 and IGS-2.

Table 2. Scenario 1

Space Object	Error (KM) 1-σ tang	ΔV (KM/Sec) for 1000 KM Acq. Dist.	
		IGS 1	IGS 2
A	10	.10604	.06053
B	20	*.17676	.10692
C	50	.14777	*.10951
D	20	.14188	.08789

Scenario 2. A 250 km acquisition sensor was used with IGS-1 and IGS-2. Table 3 shows the results. In this scenario, the largest ΔV requirements demand 133 kg of propellant and 79 kg of propellant for IGS-1 and IGS-2, respectively. In this case, the difference of 54 kg might impact the mission and influence the tradeoff.

Table 3. Scenario 2

Space Object	Error (KM) 1-σ tang	ΔV (KM/Sec) for 250 KM Acq. Dist.	
		IGS 1	IGS 2
A	10	.42417	.24213
B	20	*.70704	.42769
C	50	.59108	*.43805
D	20	.56752	.35157

Scenario 3. A 250 km acquisition sensor and IGS-4 were used. Additionally, the effect of improving the space object trading accuracy to 1 km (1-σ, tangential) was assessed. Table 4 shows the results. Using the largest ΔV requirements, a reduction of 50 kg of propellant is achieved by improving the space object

tracking accuracy.

Table 4. Scenario 3

Space Object	ΔV (KM/Sec) for 250 KM acq. Dist.	
	Previous Errors	1 KM (1-σ tang)
A	.07837	.04243
B	.19443	*.06793
C	*.33252	.04548
D	.17565	.05385

VALIDATION

There is to date no actual direct ascent, deep space intercept system. Because there are no real world performance results, model validation was achieved with the "towards-validation" approach suggested by Ghelber and Haley (2). Ghelber and Haley define the "towards validation" approach as, "the documented evidence that a computerized model can provide users verifiable insight, within the model's domain of application, for the purpose of formulating analytical or decision-making inferences" (2:13). This process involves a four phased approach: (1) conceptual, (2) verification, (3) credibility and (4) confidence. All phases were successfully accomplished. For this paper, the confidence phase is specifically described.

Ghelber and Haley contend that confidence building begins with the first steps in the conceptual phase and continues through all the previously mentioned model building and use (2:29). One of the recommended steps in this phase is a statistical comparison of modified simulation runs with related data.

In all runs of various target scenarios and guidance and target error combinations, statistical consistency of the model was achieved. The following equation was used to compute the interval about the sample mean (miss distance) within which the true mean is located to a confidence of 95%:

$$\bar{x} - \frac{1.96\sigma}{(n)^{0.5}} < \mu < \bar{x} + \frac{1.96\sigma}{(n)^{0.5}}$$

where $\bar{x}$ is the sample mean
μ is the true mean
σ is sample standard deviation
n is the sample size

The runs conducted in this analysis consistently showed the true mean to be within 0.1% of the sample mean. Table 5 shows a sample of results.

CONCLUSIONS

A model has been developed for evaluating error contributions within a direct ascent, deep space intercept system. It is a model which can be used as an aid in assessing the overall system performance.

Table 5.
Sample Results for Test of Sample Means (95% Confidence)

Space Object	IGS#	Target Error (1σ tang)	% Deviation
A	1	1 KM	.07
A	3	20 KM	.06
B	2	50 KM	.05
C	4	100 KM	.07
D	1	100 KM	.06

BIBLIOGRAPHY

1. Bate, Roger R., Donald D. Mueller, and Jerry E. White. Fundamentals of Astrodynamics. New York: Dover Publications, Inc., 1971.

2. Ghelber, Craig S. and Charles A. Haley. "A methodology for Validation of Complex Multi-Variable Military Models." Unpublished MS Thesis, School of Engineering, Air Force Institute of Technology, Wright-Patterson AFB, Ohio, 1980.

3. Sridrahan, S. and W. Sinieu. Deep Space Group, MIT Lincoln Laboratory. Telephone interviews 27 and 29 July 1983.

4. Stark, Peter A. Introduction to Numerical Methods. New York: The Macmillan Company, 1970.

5. Vandergraft, James S. Introduction to Numerical Computations. New York: The Academic Press, 1978.

6. Whitcomb, David W. Personal Correspondence. The Aerospace Corporation, Los Angeles, CA, 4 August 1983.